

## Modelling of Non-Premixed Turbulent Combustion of Hydrogen using Conditional Moment Closure Method

This article has been downloaded from IOPscience. Please scroll down to see the full text article.

2012 IOP Conf. Ser.: Mater. Sci. Eng. 36 012036

(<http://iopscience.iop.org/1757-899X/36/1/012036>)

View [the table of contents for this issue](#), or go to the [journal homepage](#) for more

Download details:

IP Address: 139.86.2.14

The article was downloaded on 18/09/2012 at 12:09

Please note that [terms and conditions apply](#).

# Modelling of Non-Premixed Turbulent Combustion of Hydrogen using Conditional Moment Closure Method

M.M.Noor<sup>1,3</sup>, A.Aziz Hairuddin<sup>1,4</sup>, Andrew P.Wandel<sup>1</sup> and T.F.Yusaf<sup>2,3</sup>

<sup>1</sup>Computational Engineering and Science Research Centre, Department of Mechanical and Mechatronic, Engineering University of Southern Queensland (USQ), Australia

<sup>2</sup>National Centre for Eng. in Agriculture (NCEA), USQ, Australia

<sup>3</sup>Faculty of Mechanical Engineering, Universiti Malaysia Pahang (UMP), Malaysia

<sup>4</sup>Faculty of Engineering, Universiti Putra Malaysia (UPM), Malaysia

E-mail: Muhamad.MatNoor@usq.edu.au / muhamad@ump.edu.my

**Abstract.** Most of the electricity generation and energy for transport is still generated by the conversion of chemical to mechanical energy by burning the fuels in the combustion chamber. Regulation for pollution and the demand for more fuel economy had driven worldwide researcher to focus on combustion efficiency. In order to reduce experimental cost, accurate modelling and simulation is very critical step. Taylor series expansion was utilised to reduce the error term for the discretization. FORTRAN code was used to execute the discretized partial differential equation. Hydrogen combustion was simulated using Conditional Moment Closure (CMC) model. Combustion of hydrogen with oxygen was successfully simulated and reported in this paper.

## 1. Introduction

Energy is a human basic need. Currently, combustion remains the main source of energy for transportation, industrial, electricity generation and other human activities. World energy demand for 2030 is estimated at about 18 billion tons of oil equivalent and about 80 percent will be fulfilled by oil, gas and coal [1,2]. Worldwide concern on fuel prices, environmental pollution and energy sustainability has led to an increased interest in energy efficiency improvement with lower emissions. This issue has driven the combustion community to focus on the research for experimental and modelling. Turbulent combustion is divided into two classes depending on when the fuel is mixed with the oxidizer: premixed and non-premixed. Premixed combustion is usually modelled using eddy break-up model, coherent flame, flamelet based on G-equation or linear eddy model. However, premixed combustion is not of interest of this paper. For non-premixed combustion, there are a few types of modelling methods for the mixing process: probability density function (PDF) based model [3-5], flamelet model [6-9], fast chemistry limit model [10], and mapping closure model [11,12]. Besides those models, there are a few other developments such as conditional moment closure (CMC) by Klimenko and Bilger [13-15] and multiple mapping conditioning (MMC) by Klimenko and Pope [16], with further developments [17-20] for the mixing process. The CMC model for non-premixed combustion will be investigated in this paper.

The concept of turbulent combustion modelling describes the transport of reactive scalars in conserved scalar spaces. The novelty of CMC model was the capability of the model to take into account the conditional averages in the combustion modelling. This is due to the chemical source term is not a function of unconditional averages, which are used in conventional modelling. Ternat et al [21] computed stable solutions using two finite difference methods, namely the Euler method and the Crank–Nicolson method, to advance the solution of the heat equation in time. Noor et al [22] use Taylor expansion to discretize the CMC model and finite difference method to solve the equation through explicit and implicit method. Clarke et al [23] used direct numerical simulation (DNS) results to model the parameters of CMC for combustion systems with droplets. This is a complicated process because of the interaction of the evaporating liquid with the gaseous phase; the usage of a spark to evaporate the fuel and ignite the mixture exacerbates this complexity in comparison with auto ignition.

A mixing model is required to close the molecular diffusion term in the PDF transport equation [3], which is the last term in equation (1) and contains the molecular diffusion flux vector ( $J_{ik}$ ):

$$\begin{aligned} \bar{\rho} \frac{\partial \tilde{P}(\underline{\psi})}{\partial t} + \bar{\rho} \tilde{u}_m \frac{\partial \tilde{P}(\underline{\psi})}{\partial x_m} + \bar{\rho} \sum_{k=1}^n \frac{\partial}{\partial \psi_k} \{ \dot{\omega}_k(\underline{\psi}) \tilde{P}(\underline{\psi}) \} = - \frac{\partial}{\partial x_m} \{ \bar{\rho} \langle u_k'' | \underline{\phi} = \underline{\psi} \rangle \} \tilde{P}(\underline{\psi}) \\ + \sum_{k=1}^n \frac{\partial}{\partial \psi_k} \left\{ \left\langle \frac{\partial J_{i,k}}{\partial x_i} \right|_{\underline{\phi} = \underline{\psi}} \right\} \tilde{P}(\underline{\psi}) \end{aligned} \quad (1)$$

Mixing plays a crucial role in the non-premixed combustion process; a number of mixing models have been developed. The Coalescence and Dispersion process was modelled by Curl in 1963 [24] and Levenspiel and Spielman in 1965 [25] and is often called ‘‘Curl’s model’’. The governing equation for Curl’s model is shown in equation (2). The left part of the equation is the particle composition before mixing. This particle then Coalescences with another particle and mixing occurs. The mixing process can be referred to at the middle part of equation (2) and then this mixed particle will be dispersed as shown in the last part of equation (2).

$$\left( \begin{array}{l} (\phi_{A1}, \phi_{B1})_1 \\ (\phi_{A2}, \phi_{B2})_2 \end{array} \right) \rightarrow \left( \begin{array}{l} \phi_A^* = (\phi_{A1} + \phi_{A2})/2 \\ \phi_B^* = (\phi_{B1} + \phi_{B2})/2 \end{array} \right) \rightarrow \left( \begin{array}{l} (\phi_A^*, \phi_B^*)_1 \\ (\phi_A^*, \phi_B^*)_2 \end{array} \right) \quad (2)$$

Here  $\phi_{A1}$  is the composition of species A for particle 1,  $\phi_A^*$  is the new composition of species A and  $(\phi_A, \phi_B)$  is a particle which consists of species A and B. The Curl’s model was modified by Janicka et. al [26] and Dopazo [27] in 1979. This model was called modified Curl’s (MC) model (equations (3) and (4)) where  $\beta$  can take any value from 0 to 1 and can be a random variable. If  $\beta = 0$ , then no mixing occurs, whilst  $\beta = 1$  reproduces Curl’s model.

$$\phi_i^{MC}(t + \delta t) = (1 - \beta t) \phi_i^{MC}(t) + \frac{1}{2} \beta \left( \phi_j^{MC}(t) + \phi_i^{MC}(t) \right) \quad (3)$$

$$\phi_j^{MC}(t + \delta t) = (1 - \beta t) \phi_j^{MC}(t) + \frac{1}{2} \beta \left( \phi_j^{MC}(t) + \phi_i^{MC}(t) \right) \quad (4)$$

Here  $\phi_i$  and  $\phi_j$  is the composition of particles  $i$  and  $j$ ,  $t$  is time and  $\delta t$  is the time interval.

The weakness of the MC model is that this mixing process does not enforce the requirement that only particles that are close to each other are allowed to mix and interact with each other. This issue was solved by the Euclidean Minimum Spanning Tree (EMST) model [28] whereby particles that mix are close together in composition space as shown in equations (5) and (6). In these equations, there are two new constants introduced where  $d$  is determined so that the desired amount of mixing is obtained and  $P_b$  is the position of particle in the EMST branch. Particles near to the centre will have higher  $P_b$  values.

$$\phi_i^{EMST}(t + \delta t) = \phi_i^{EMST}(t) + dP_b \delta t (\phi_j^{EMST}(t) + \phi_i^{EMST}(t)) \quad (5)$$

$$\phi_j^{EMST}(t + \delta t) = \phi_j^{EMST}(t) + dP_b \delta t (\phi_i^{EMST}(t) + \phi_j^{EMST}(t)) \quad (6)$$

Another mixing model is the interaction by exchange with the mean (IEM) model [29] where the composition of all particles in a cell are moved a small distance toward the mean composition using a characteristic mixing timescale. The IEM equation is shown in equation (7) where  $\tilde{\phi}$  is the Favre mean-composition vector at the particle's location and  $\tau_t$  is the turbulence time scale. The scalar mixing time scale  $\tau_\phi$  in equation (7) is often modelled as proportional to  $\tau_t$  as in equation (8).

$$\frac{\partial \phi}{\partial t} = -\frac{\phi - \tilde{\phi}}{2\tau_\phi} \quad (7)$$

$$\tau_\phi \equiv \frac{\tau_t}{c_\phi} \quad (8)$$

The mixing models just described are either non-local [24-27] or over-local [28], thereby producing imperfect combustion modelling processes. Recently Wandel [30] has proposed a new mixing model which randomizes the particle interaction in a local manner. The proposed model is the Stochastic Particle Diffusion Length (SPDL) [30] model, which is based upon the practical localness of the random inter-particle distance [31].

Combustion processes are very complex especially because the chemical reactions between chemical species involved in burning fuel (gas, liquid or solid) are highly non-linear functions of temperature and species concentration. Significant errors are produced when a computational fluid dynamics (CFD) code only solves the Reynolds Averaged Navier-Stokes (RANS) model as written in equation (9), which involves averaging the source terms. All terms are averaged and the models work reasonably well when solving  $\bar{\phi}$  for velocity but not for chemical species.

$$\frac{\partial \bar{\rho} \bar{\phi}}{\partial t} + \frac{\partial \bar{\rho} \bar{\phi} \bar{u}_i}{\partial x_i} = \frac{\partial}{\partial x_i} \left[ D \frac{\partial \bar{\phi}}{\partial x_i} \right] + \bar{W} + \bar{T} \quad (9)$$

These models are inaccurate and produce errors by ignoring the correlation between the source term variables, which are generally significant, compared to the corresponding averages. These errors were overcome by the CMC model using the conditional averages method. It takes the average of the variables for a specified value of the mixture fraction and effectively averages over a smaller region of space. Compare to the IEM and EMST model, CMC is more accurate at the cost of more complex simulations that require more computational time. The chemical source term  $\langle W|Z \rangle$  can be calculated using equation (10) and the reaction rate is obtained by using equation (11). The Arrhenius equation [18] in equation (12) is used to determine the reaction rate constant. The chemical source term, reaction rate and reaction rate constant can be written as:

$$W_I = \frac{w_I}{\rho} \sum_j v_{Ij} \omega_j \quad (10)$$

$$\omega_j = \left[ k_{fj} \prod_{l=1}^{n_s} [X_l]^{v'_{lj}} - k_{bj} \prod_{l=1}^{n_s} [X_l]^{v''_{lj}} \right] \quad (11)$$

$$k = AT^\beta \exp\left(-\frac{E_a}{RT}\right) \quad (12)$$

with the rate of progress variable  $\omega_j$  the net strength of reaction  $j$  in the forward direction,  $w_I$  is the mean molecular weight,  $\rho$  is density,  $E_a$  is the activation energy,  $A$  and  $\beta$  are Arrhenius constants,  $R$  is

the ideal gas constant, and  $T$  is temperature. The CMC equation for two-phase homogenous systems is shown in equation (13):

$$\frac{\partial \langle Y|Z \rangle}{\partial t} = \langle N|Z \rangle \frac{\partial^2 \langle Y|Z \rangle}{\partial Z^2} + \langle W|Z \rangle + \langle S|Z \rangle \quad (13)$$

The combustion of hydrogen produces the most clean and very low emission in combustion. Hydrogen's low density giving a challenging medium for the storage (requires very high pressure tank). Table 1 shows the properties of natural gas, hydrogen and diesel.

**Table 1** Diesel properties compared to hydrogen and natural gas [32-35]

Properties	Diesel	Hydrogen	Natural Gas
Main component	C and H	H Only	Methane (CH <sub>4</sub> )
Auto-ignition Temperature (K)	553	858	923
Lower heating value (MJ/kg)	42.5	119.93	50
Density (kg/m <sup>3</sup> )	833-881	0.08	692
Molecular weight (g/mol)	170	2.016	16.043
Flammability limits in air (vol %)	0.7-5	4-75	5-15
Flame velocity (m/s)	0.3	2.65-3.25	0.45
Specific gravity	0.83	0.091	0.55
Boiling point (K)	453-653	20.2	111.5
Cetane number	40-60	-	-
Octane number	30	130	120
CO <sub>2</sub> emissions (%)	13.4	0	9.5
Mass diffusivity in air (cm <sup>2</sup> /s)	-	0.61	0.16
Min ignition energy (mJ)	-	0.02	0.28

Fuel blend with hydrogen additive will increase the molecular diffusion with the increase of hydrogen [36]. Recently Mardani et al. [36,37] and Wang et al. [38] investigated the effects of hydrogen addition and found that flameless combustion occurred more easily. Yu et al. [39] found that pure hydrogen could not reduce thermal NO<sub>x</sub> emission in the flameless combustion regime. Hydrogen properties show a lot of advantage over fossil fuels. Hydrogen is produced mainly from fossil fuel resources and only 4% generated by electrolysis. In the future, when fossil fuel depleted, the raw material will be changed to water and biomass [40]. The important properties that serve best for combustion are: high auto-ignition temperature. The higher auto-ignition temperature allows higher compression ratio and produce higher engine thermal efficiencies; high diffusivity. More homogenous combustion due to more uniform air-fuel mixture and will disperse quickly if leaking; wide range of flammability. Fuel air mixing ratios from 4% to 74% and can be burned on a lean mixture with fuel economy and produce less NO<sub>x</sub>. The disadvantage is the power produced will be significantly lower than fossil fuel; low ignition energy. To ignite, hydrogen only needs 10% of what gasoline needs. The disadvantage is possible early ignition causing knocking problems; low density leads to low energy density and larger storage; high flame velocity requires tighter ignition timing and burns at about 2.83 m/s compare to 0.34 m/s for gasoline (at stoichiometric and atmospheric pressure).

In this paper, Taylor series expansion method was utilised to discretise the CMC equation and FORTRAN code was used to run a simulation and produce results. The purpose of the study is to simulate the reaction of hydrogen and oxygen using CMC mixing model. Explicit and implicit method was used and the outcome from both methods will be discussed.

## 2. Taylor Expansion

Numerical method is very important to reduce the experimental cost. After simulation results are obtained and ready to be validated, then experimentation is used to confirm the findings and results from the simulation. There are many numerical methods can be utilized to solve partial differential equation (PDE). Implicit and explicit methods are the common methods. Implicit finite difference relations have been derived by many mathematicians and physicists with various methods [41-53]. Most of them claim that all the implicit formulas can be derived from a Taylor series expansion. The Taylor series expansion is a good basis for studying numerical methods since it provides a means to predict a function's value at one point in terms of the function's value and derivatives at another point. In particular, the theorem states that any smooth function can be approximated as a polynomial [53]. There are many different types of numerical differentiation formulations, depending on the number of points, direction of the formula and the required derivative order [54]. The Taylor expansion is a useful method to discretise partial differential equations to minimise and accurately predict the value of the error term. The expansions for  $y_1$  and  $y_{-1}$  which are to the right and to the left of  $y_0$  respectively are shown below up to the 7<sup>th</sup>-order derivatives as equations (14) and (15).

$$y_1 = y_0 + (\Delta x_1) \frac{dy}{dx} \Big|_{x_0} + \frac{(\Delta x_1)^2}{2!} \frac{d^2 y}{dx^2} \Big|_{x_0} + \frac{(\Delta x_1)^3}{3!} \frac{d^3 y}{dx^3} \Big|_{x_0} + \frac{(\Delta x_1)^4}{4!} \frac{d^4 y}{dx^4} \Big|_{x_0} + \frac{(\Delta x_1)^5}{5!} \frac{d^5 y}{dx^5} \Big|_{x_0} + \frac{(\Delta x_1)^6}{6!} \frac{d^6 y}{dx^6} \Big|_{x_0} + \frac{(\Delta x_1)^7}{7!} \frac{d^7 y}{dx^7} \Big|_{x_0} \quad (14)$$

$$y_{-1} = y_0 + (\Delta x_{-1}) \frac{dy}{dx} \Big|_{x_0} + \frac{(\Delta x_{-1})^2}{2!} \frac{d^2 y}{dx^2} \Big|_{x_0} + \frac{(\Delta x_{-1})^3}{3!} \frac{d^3 y}{dx^3} \Big|_{x_0} + \frac{(\Delta x_{-1})^4}{4!} \frac{d^4 y}{dx^4} \Big|_{x_0} + \frac{(\Delta x_{-1})^5}{5!} \frac{d^5 y}{dx^5} \Big|_{x_0} + \frac{(\Delta x_{-1})^6}{6!} \frac{d^6 y}{dx^6} \Big|_{x_0} + \frac{(\Delta x_{-1})^7}{7!} \frac{d^7 y}{dx^7} \Big|_{x_0} \quad (15)$$

We assume  $\Delta_i$  is constant, then  $y_1$  and  $y_0$  become

$$y_1 = y_0 + (\Delta x) \frac{dy}{dx} \Big|_{x_0} + \frac{(\Delta x)^2}{2!} \frac{d^2 y}{dx^2} \Big|_{x_0} + \frac{(\Delta x)^3}{3!} \frac{d^3 y}{dx^3} \Big|_{x_0} + \frac{(\Delta x)^4}{4!} \frac{d^4 y}{dx^4} \Big|_{x_0} + \frac{(\Delta x)^5}{5!} \frac{d^5 y}{dx^5} \Big|_{x_0} + \frac{(\Delta x)^6}{6!} \frac{d^6 y}{dx^6} \Big|_{x_0} + \frac{(\Delta x)^7}{7!} \frac{d^7 y}{dx^7} \Big|_{x_0} \quad (16)$$

$$y_{-1} = y_0 + (\Delta x) \frac{dy}{dx} \Big|_{x_0} + \frac{(\Delta x)^2}{2!} \frac{d^2 y}{dx^2} \Big|_{x_0} + \frac{(\Delta x)^3}{3!} \frac{d^3 y}{dx^3} \Big|_{x_0} + \frac{(\Delta x)^4}{4!} \frac{d^4 y}{dx^4} \Big|_{x_0} + \frac{(\Delta x)^5}{5!} \frac{d^5 y}{dx^5} \Big|_{x_0} + \frac{(\Delta x)^6}{6!} \frac{d^6 y}{dx^6} \Big|_{x_0} + \frac{(\Delta x)^7}{7!} \frac{d^7 y}{dx^7} \Big|_{x_0} \quad (17)$$

Rearrangement of equations (16) and (17) becomes the first order derivatives at  $x_0$  as below (equations (18), (19) and (20)). Equation (16) is used to obtain the forward difference method (which calculates  $\frac{dy}{dx} \Big|_{x_0}$  based on forward movement from  $y_0$  to  $y_1$ ):

$$\frac{dy}{dx} = \frac{(y_1 - y_0)}{\Delta x} - \frac{(\Delta x)}{2!} \frac{d^2 y}{dx^2} - \frac{(\Delta x)^2}{3!} \frac{d^3 y}{dx^3} - \frac{(\Delta x)^3}{4!} \frac{d^4 y}{dx^4} - \frac{(\Delta x)^4}{5!} \frac{d^5 y}{dx^5} - \frac{(\Delta x)^5}{6!} \frac{d^6 y}{dx^6} - \frac{(\Delta x)^6}{7!} \frac{d^7 y}{dx^7} \quad (18)$$

Equation (17) is used to obtain the backward difference method, which calculates  $\frac{dy}{dx} \Big|_{x_0}$  based on backward movement from  $y_0$  to  $y_{-1}$ .

$$\frac{dy}{dx} = \frac{(y_0 - y_{-1})}{\Delta x} - \frac{(\Delta x)}{2!} \frac{d^2 y}{dx^2} - \frac{(\Delta x)^2}{3!} \frac{d^3 y}{dx^3} - \frac{(\Delta x)^3}{4!} \frac{d^4 y}{dx^4} - \frac{(\Delta x)^4}{5!} \frac{d^5 y}{dx^5} - \frac{(\Delta x)^5}{6!} \frac{d^6 y}{dx^6} - \frac{(\Delta x)^6}{7!} \frac{d^7 y}{dx^7} \quad (19)$$

By taking the difference between equations (16) and (17), the central difference method is derived which calculates  $\left. \frac{dy}{dx} \right|_{x_0}$  based on the domain between  $y_1$  and  $y_{-1}$

$$\frac{dy}{dx} = \frac{(y_1 - y_{-1})}{2\Delta x} - \frac{(\Delta x)^2}{3!} \frac{d^3 y}{dx^3} - \frac{(\Delta x)^4}{5!} \frac{d^5 y}{dx^5} - \frac{(\Delta x)^6}{7!} \frac{d^7 y}{dx^7} \quad (20)$$

with leading error term of  $\frac{(\Delta x)^2}{6!} \frac{d^3 y}{dx^3}$ . This equation (20) is a second-order accurate method:  $O(\Delta x^2)$ . Since the differences actually evaluate the derivative at the midpoint of the finite difference, equation (20) estimates the derivative at  $x_0$ , while equation (18) and (19) estimate the derivative either side of  $x_0$ . Using central difference derivative, we can obtain  $\frac{d^2 y}{dx^2}$  from equations (16) and (17), as shown in equation (21). The first term in equation (21) can be re-arranged as equation (22) to show that this is simply a central difference of the first derivative.

$$\frac{d^2 y}{dx^2} = \frac{(y_1 - 2y_0 + y_{-1})}{(\Delta x)^2} - \frac{2!(\Delta x)^2}{4!} \frac{d^4 y}{dx^4} - \frac{2!(\Delta x)^4}{6!} \frac{d^6 y}{dx^6} \quad (21)$$

$$= \frac{1}{\Delta x} \left( \frac{y_1 - y_0}{\Delta x} - \frac{y_0 - y_{-1}}{\Delta x} \right) \quad (22)$$

The leading error term is  $\frac{(\Delta x)^2}{12!} \frac{d^4 y}{dx^4}$ , so this is a second-order accurate method:  $O(\Delta x^2)$ . The first-order derivative using the fourth-order Taylor expansion scheme is below, for the difference between  $y_2$  and  $y_{-2}$ :

$$\frac{dy}{dx} = \frac{(y_{-2} - 8y_{-1} + 8y_1 - y_2)}{12\Delta x} + \frac{4(\Delta x)^4}{5!} \frac{d^5 y}{dx^5} \quad (23)$$

with leading error term of  $\frac{(\Delta x)^4}{30} \frac{d^5 y}{dx^5}$ . This is a fourth-order accurate method:  $O(\Delta x^4)$  and can be summarized as equation (24) to show that it is a weighted average of the “near” and “far” central differences:

$$\frac{dy}{dx} = \left( \frac{4}{3} \right) \frac{(y_1 - y_{-1})}{(2\Delta x)} - \left( \frac{1}{3} \right) \frac{(y_2 - y_{-2})}{(4\Delta x)} \quad (24)$$

The second-order derivative for the fourth-order Taylor expansion scheme is equation (25):

$$\frac{d^2 y}{dx^2} = \frac{(-y_{-2} + 16y_{-1} - 30y_0 + 16y_1 - y_2)}{12(\Delta x)^2} + \frac{8(\Delta x)^4}{6!} \frac{d^6 y}{dx^6} \quad (25)$$

with leading error term of  $\frac{(\Delta x)^4}{90} \frac{d^6 y}{dx^6}$ , so this is a fourth-order accurate method:  $O(\Delta x^4)$ . This can be summarized as equation (26):

$$\frac{d^2 y}{dx^2} = \left( \frac{4}{3} \right) \frac{(y_{-1} - 2y_0 + y_1)}{(\Delta x)^2} - \left( \frac{1}{3} \right) \frac{(y_{-2} - 2y_0 + y_2)}{(2\Delta x)^2} \quad (26)$$

Interestingly, the weightings of the terms in equation (26) for the second-order derivative are identical to those in equation (24) for the first-order derivative. The third-order derivative for the second-order Taylor expansion scheme is shown as equation (27):

$$\frac{d^3 y}{dx^3} = \frac{(-y_{-2} - 2y_{-1} - 2y_1 + y_2)}{2(\Delta x)^3} - \frac{(\Delta x)^2}{4} \frac{d^5 y}{dx^5} \quad (27)$$

with leading error term of  $\frac{(\Delta x)^2}{4} \frac{d^5 y}{dx^5}$ , so this is a second-order accurate method:  $O(\Delta x^2)$ .

Assuming that there is a uniform spacing of  $\Delta x$ , using notation that  $y^{(k)} = \frac{d^k y}{dx^k}$ , for the Taylor series expansion, central difference derivatives can be summarised as equation (28):

$$y^{(k)} = C \sum_{i=-\frac{(n-1)}{2}}^{\frac{(n-1)}{2}} z_i y_i + ET \quad (28)$$

Forward difference derivatives can be written as equation (29):

$$y^{(k)} = C \sum_{i=0}^{(n-1)} z_i y_i + ET \quad (29)$$

Backward difference derivatives can be written as equation (30):

$$y^{(k)} = C \sum_{i=-(n-1)}^0 z_i y_i + ET \quad (30)$$

where  $n$  is the number of points ( $y_{-2}, y_{-1}, y_0, y_1, y_2$  is equal to five points),  $ET$  is the leading error term and  $z_i$  is the coefficient of  $y$  for each point  $i$ .

### 3. Numerical Method

The finite difference schemes, as agreed by most of the scientific community, were first used by Euler (1707-1783) [55] to find an approximate solution of a differential equation. It was invented prior to boundary element methods (BEM), finite element methods (FEM), spectral methods, and discontinuous spectral element methods [56]. FDM is still relevant and remain competitive as a discretisation method for use in many applications and can be used to solve problems with simple and complex geometry, such as fluid flows and gas reaction [57,58]. The Finite difference method (FDM) is a numerical method for approximating the solutions to partial differential equations by using finite difference equations to approximate derivatives based on the properties of Taylor expansions and on the straightforward application of the definition of derivatives [59]. The objectives are to transform the calculus problem to algebra as from a continuous equation to a discrete equation. The discretisation process is a mathematical process that divides the continuous physical domain into a discrete finite difference grid and then approximates each individual partial derivative in the partial differential equation. Using the Taylor expansion method, a partial differential equation was discretised in order to transform it to FORTRAN code. FORTRAN is a high level of programming language developed by team of IBM programmers led by John Backus in 1954. The name of FORTRAN was derived from the words "Formula Translation", started from 1957 when the first FORTRAN compiler was used. It has evolved through FORTRAN II, FORTRAN 66, until now FORTRAN 2008. FORTRAN 90 was used in this study. From the CMC equation, to study the discretisation and code it in FORTRAN, simplifications of the CMC equation were used: the conditional chemical source term ( $\langle W|Z \rangle$ ) and conditional generation due to droplet evaporation term ( $\langle S|Z \rangle$ ) were not considered. So the homogeneous and passive CMC is equation (31):

$$\frac{\partial \langle Y|Z \rangle}{\partial t} = \langle N|Z \rangle \frac{\partial^2 \langle Y|Z \rangle}{\partial z^2} \quad (31)$$

In this equation, the conditional mass fraction quantity  $\langle Y|Z \rangle$  can be considered as "Y is a function of Z" (written as  $y(Z)$ ) and conditional scalar dissipation  $\langle N|Z \rangle$  is expressed as "N is a function of Z" (written as  $N(Z)$ ). After summarizing all the assumption, the CMC equation becomes equation (32):



$$\frac{dy}{dt} = N \frac{d^2y}{dz^2} \quad (32)$$

The Taylor expansion equations (18) and (21) can be expressed in this nomenclature as:

$$\frac{dy}{\partial t} = \frac{y(z,t+\Delta t) - y(z,t)}{(\Delta t)} \quad (33)$$

$$\frac{d^2y}{\partial z^2} = \frac{y(z+\Delta z,t) - 2y(z,t) + y(z-\Delta z,t)}{(\Delta z)^2} \quad (34)$$

The final form of the CMC equation after discretization is represented by equation (35) for the explicit method and equation (36) for implicit.

$$YH(i, j + 1) = \left( (1 - (2B)) * YH(i, j) \right) + (B * YH(i + 1, j)) + (B * YH(i - 1, j)) \quad (35)$$

$$(1 + 2B) * YH(i, j + 1) - (B * YH(i + 1, j + 1)) - (B * YH(i - 1, j + 1)) = YH(i, j) \quad (36)$$

where  $B = N \frac{\Delta t}{(\Delta z)^2}$ ,  $YH$  is the array in the computer code for the variable mass fraction of fuel,  $i$  is the index for mixture fraction and  $j$  is the index of the time step. Equations (35) and (36) were coded in FORTRAN to simulate the CMC modelling. Parts of the FORTRAN code for the explicit and implicit methods are listed in appendixes A and B.

Three parameters were used as input to the code:  $dt$  is time step size,  $dz$  is step size in mixture fraction space and  $TT$  is total time for the simulation. These three parameters will determine the accuracy and total time taken to run the code. The more steps taken, the longer it will take to complete the simulation. The result of the simulation must be checked to ensure its convergence meets expectations. These parameter must also comply with the Courant-Friedrichs-Lewy (CFL) condition [60,61] to ensure the stability of the solution and that the result acceptably reaches a converged solution. The stability of the solution is very important because an unstable condition will create large errors in the solution and wrong predictions of the result. The time-step must satisfy the condition shown in equation (37) otherwise the simulation will produce incorrect results.

$$CFL = N \frac{dt}{dz^2} \leq \frac{1}{2} \quad (37)$$

In order to achieve this condition, the time step must be small enough for the flow conditions.

#### 4. Results and Discussions

In this study, the value for the conditional scalar dissipation  $N$  in was assumed to be the constant 0.5. Results from the simulation are plotted in Figures 1. The explicit method was found to converge faster than the implicit method, reaching the steady-state condition after 190 time steps whereas implicit required 247 time steps. ("Steady-state" is defined as no variation in 5 significant figures.) In addition, the time required for the computer to calculate one time step was significantly shorter for the explicit method. However, the explicit method reaches the steady-state too quickly due to greater errors in this method for the same time-step. The implicit method can have a bigger time-step ( $\delta t$ ) for the same accuracy as the explicit method.

The first lines (from  $Y = 1.0$  to  $0.0$  over the gap of  $Z = 0.1$ ) are the initial conditions that oxidizer (left lines) is zero everywhere except at  $Z = 0$  and fuel (right lines) is zero everywhere except at  $Z = 1$ . The cell size used here is  $Z = 0.1$ , which is why the line drops at both edges for both methods. The explicit and implicit methods start to show changes for both air and fuel mass fraction immediately

(after the first time step: the second lines in Figure 1). For the explicit method at mixture fraction equal to 0.2, mass fraction is still 0.00 whereas for the implicit method, for mixture fraction equal to 0.2, mass fraction values are between 0.0 and 0.2. This variation is because differences between adjacent cells in the explicit method can only march one cell at a time, while the difference influences all cells immediately in the implicit method. Because of this, the explicit method influences the adjacent cell too much, which results in the method reaching steady-state quicker. These mixing processes were repeated over many time steps. The mixing process will reach steady-state and equilibrium when both air and fuel completely mix with both reaching 0.5 at mixture fraction equal to 0.5 (Figure 1(b) and Figure 1(d)).

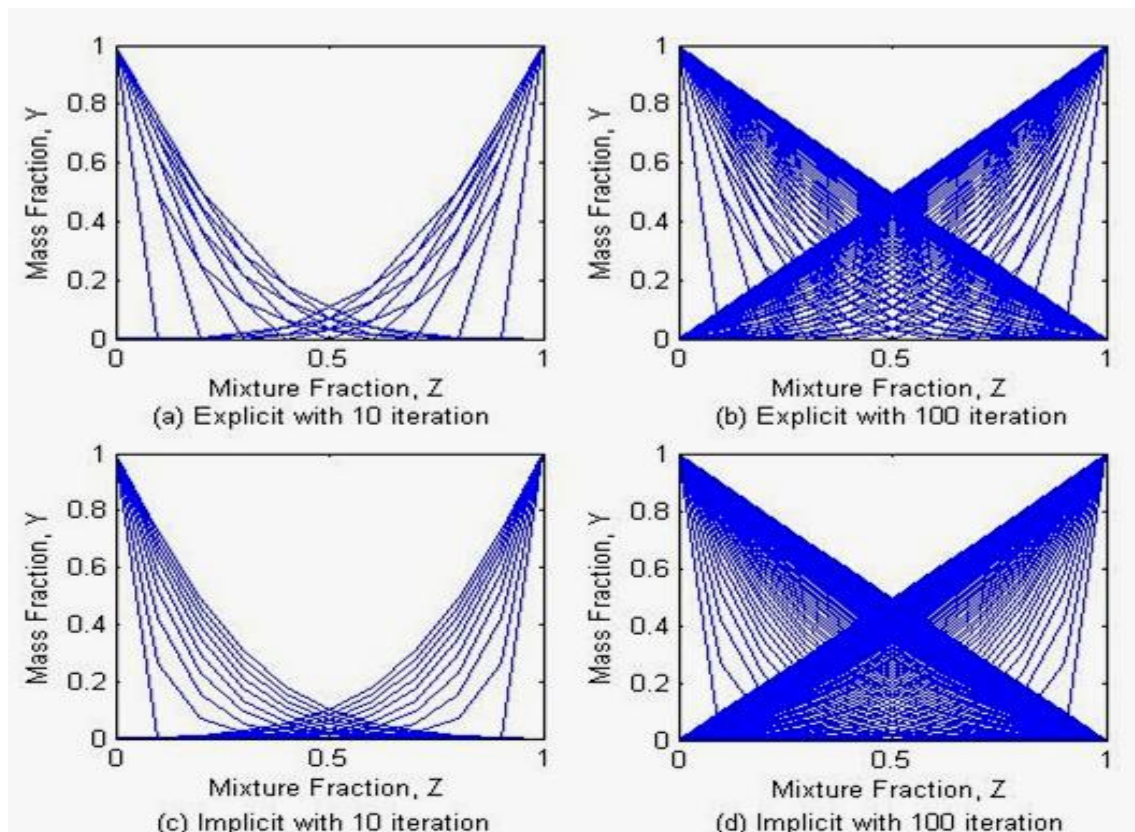


**Figure 1.** CMC mass fraction vs mixture fraction for iteration 10 and 100 for explicit and implicit method

The mixing behaviour between fuels and oxidisers in the previous discussion was studied without combustion process. Next step of this study is taking into account the combustion effect in addition to the mixing process, and after certain time, the mixing behaves differently compared to without combustion. A one-step chemical reaction of hydrogen react with oxygen was used to study the effect of combustion, which is represented in the following formula:



The combustion effect was studied in a closed system, with the same amount of initial volume. The change in mass fraction due to the chemical reaction is given by:

$$\frac{\partial Y_i}{\partial t} = \frac{w_i}{\rho} \sum_j v_{Ij} \omega_j \quad (39)$$

where,  $Y$  is the mass fraction,  $I$  is the species,  $W$  is the molecular weight,  $\rho$  is the density,  $v_{Ij}$  is the stoichiometric coefficient for species  $I$  in reaction  $j$  and  $\omega_j$  is the reaction rate. The overall stoichiometric coefficient of a chemical reaction is:

$$v_{Ij} = v_{Ij}'' - v_{Ij}' \quad (40)$$

where  $v_{Ij}''$  is the stoichiometric coefficient of product and  $v_{Ij}'$  is the stoichiometric coefficient of reactant. The reaction rate is given by:

$$\omega_j = \left[ k_{fj} \prod_{I=1}^{n_s} [X_I]^{v_{Ij}'} - k_{bj} \prod_{I=1}^{n_s} [X_I]^{v_{Ij}''} \right] \quad (41)$$

where,  $k$  is the reaction rate coefficient with subscripts  $f$  and  $b$  represent "forward" and "backward" reaction.  $X_I$  is the mole fraction of species  $I$ . Summarise and combining equation (20) and (21), the equation (19) in its full form is represented by:

$$\frac{\partial Y_I}{\partial t} = \frac{W_I}{\rho} \sum_j \left[ (v_{Ij}'' - v_{Ij}') \left( k_{fj} \prod_{I=1}^{n_s} [X_I]^{v_{Ij}'} - k_{bj} \prod_{I=1}^{n_s} [X_I]^{v_{Ij}''} \right) \right] \quad (42)$$

where the equation (22) is used to determine the change in mass fraction of the species due to combustion. The result for the combustion effect by using explicit method is shown in Fig. 2. It shows that the fuel will consume the oxidiser if we allow time for the species to mix. The mixture is not completely mixed at 10 iterations, where it will reach steady state condition (completely mixed and chemical equilibrium) when the iterations is increased to 100.

For the results in Figs. 3 and 4, the step size in mixture fraction space ( $dz$ ) for both explicit and implicit methods for combustion is 0.01 while the time step ( $dt$ ) used is 0.0001. This is smaller (both  $dz$  and  $dt$ ) compare to the simulation without combustion where  $dz$  was reduce from 0.1 to 0.01 and  $dt$  was reduce from 0.01 to 0.0001. The reason is to achieve more stable computation and obtain an appropriate resolution when the combustion is involved in the mixing process. It can be seen from Figs. 3 and 4 that the mass fraction and the mixture fraction are different compared to without combustion (Fig. 1), after the mixing process reaches steady state condition. The result is showing significant difference in mixture fraction between fuels and oxidisers, where fuels consume some amounts of oxidisers to reach the steady state condition. The mass fraction is not completely zero at the intersection line because the effect of backward reaction. Therefore, CMC modelling would be useful to study the mixing behaviour due to chemical reactions [12,14,15].

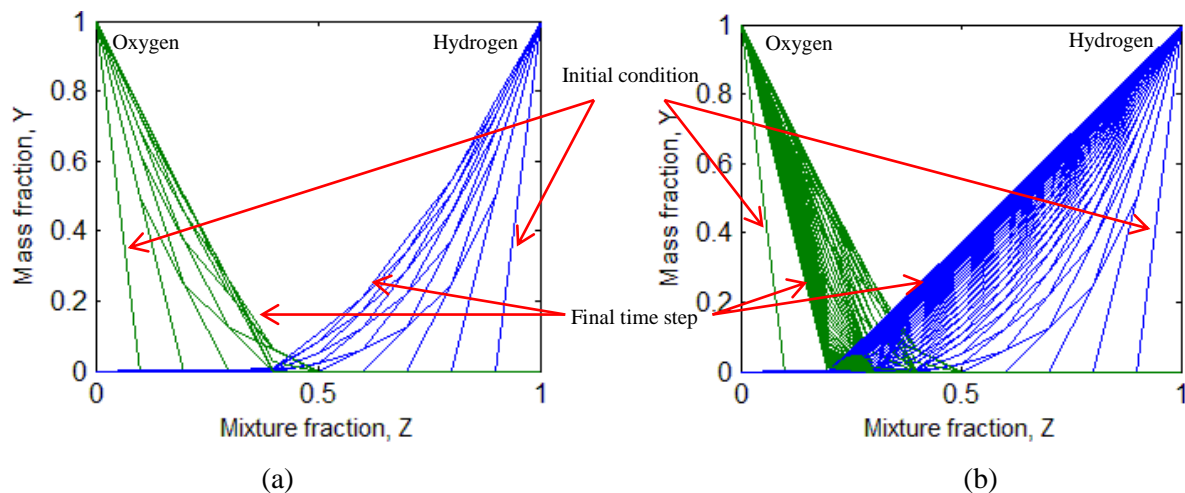


**Figure 2.** Mixing behaviour between hydrogen and oxygen for (a) 10 iterations, and (b) 100 iterations

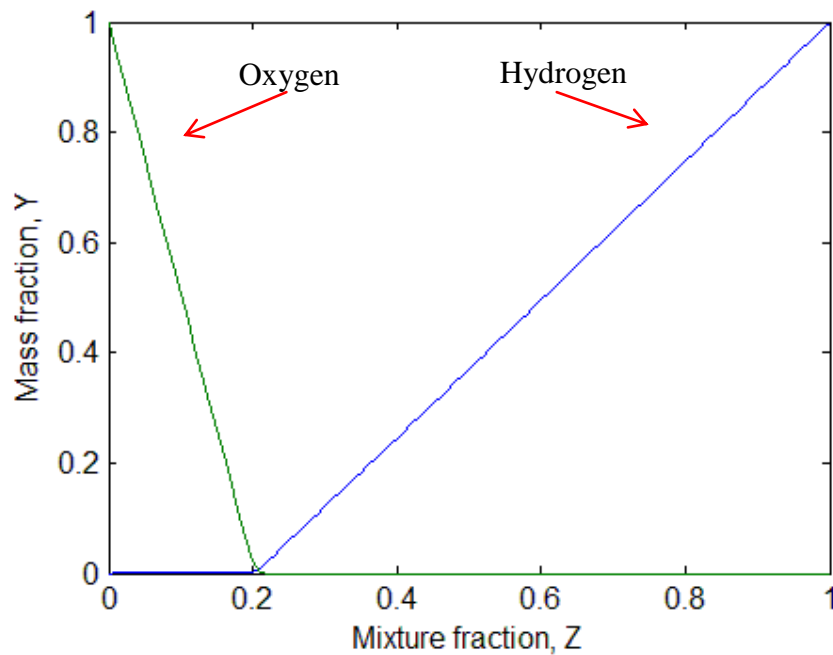


**Figure 3.** CMC simulation for mass fraction vs mixture fraction at final time step with hydrogen combustion using implicit method

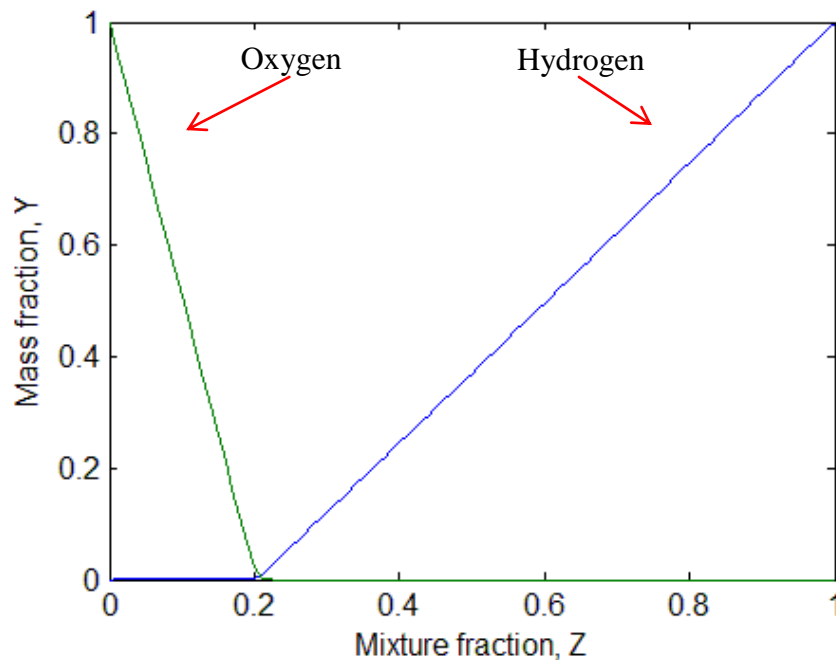


**Figure 4.** CMC simulation for mass fraction vs mixture fraction with hydrogen combustion at final time step using explicit method.

Explicit method is faster to converge than the implicit method, where the time taken for convergence for explicit method is 3867.75 s, while 4088.07 s for implicit method. The difference between the two methods at the final time step is shown in Fig. 5, where the error is small for  $Z > 0.2$ ,

which corresponds to richer compositions than the point where the mass fractions of oxygen and hydrogen intersect (Figs. 3 and 4). For the lower mixture fractions, the explicit results for both species are smaller than the implicit values, while the reverse is true where the mass fraction of hydrogen is significant. The error has its greatest magnitude near to where it changes sign on both sides of this change. A smaller time step might be required to reduce the error in this region. It seems that the explicit method is faster to converge at the expense of accuracy.

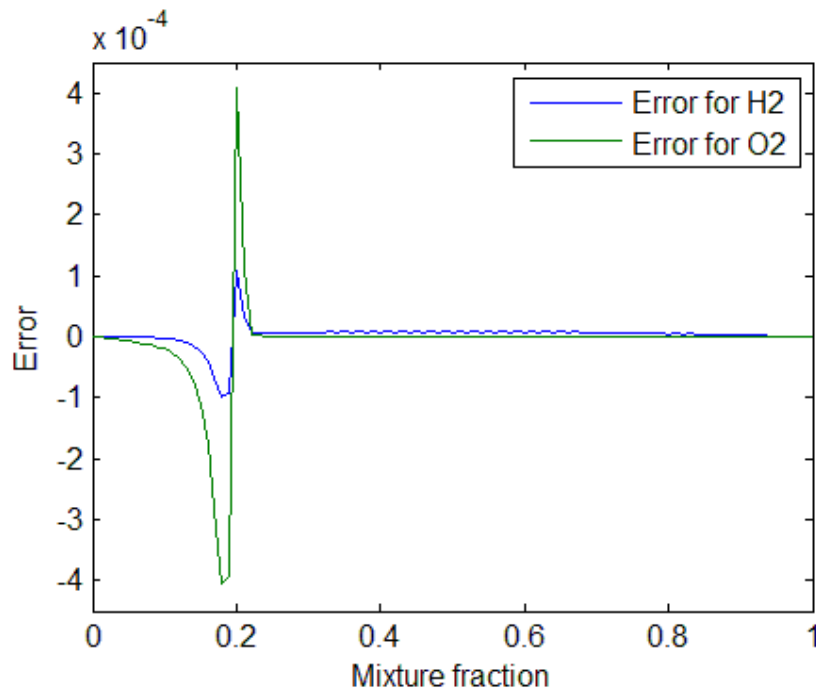


**Figure 5.** Result comparison for both oxygen and hydrogen between explicit and implicit methods at final time step. Error represents explicit – implicit.

## 5. Conclusions

The simulation process is very important to reduce high cost on the extensive experimental work. After simulation results are obtained and ready to be validated, then experimentation can take place to confirm the findings and results from the simulation. The Taylor expansion was utilized to discretize the partial differential equation for the CMC model. The modelling of CMC using explicit and implicit methods was successfully implemented using FORTRAN as the simulation software.

From the results, we conclude that the implicit method is more accurate for the same time step, whereas it is much easier to write the FORTRAN code for the explicit method and the computational time to calculate is much shorter for the same time step. When preparing to conduct simulations, the researcher needs to balance the requirements of time step size with the necessary accuracy and time required for the simulations to be run. Further work on modelling the combustion of hydrogen with oxygen using CMC was successfully carried out. From the results of the simulations, CMC modelling using FORTRAN code is very useful to analyse the mixing process and behaviour for the case of mixing coupled with chemical reactions.

## Acknowledgments

The authors would like to thank University of Southern Queensland, Universiti Malaysia Pahang and Ministry of Higher Education, Malaysia for providing laboratory facilities and financial support.

## References

- [1] IEA (International Energy Agency) Organisation for Economic Co-Operation and Development, 2009 World Energy Outlook (WEO), Int. Energy Agency, IEA, Paris
- [2] Maczulak A. 2010 'Renewable Energy, Sources and Methods', Facts on File Inc., New York, USA
- [3] Pope, SB 1985, 'PDF Methods for Turbulent Reactive Flows', Progress in Energy and Combustion Science, **11**, pp. 119-192.
- [4] Pope, SB 2000, *Turbulent Flows*, Cambridge University Press.
- [5] Haworth, DC 2010, 'Progress in Probability Density Function Methods for Turbulent Reacting Flows', Progress in Energy and Combustion Science **36**(2), pp. 168-259.
- [6] Peters, N 1980 'Local Quenching Due to Flame Stretch and Non Premixed Turbulent Combustion', Western States Section of the Combustion Inst., spring meeting, Paper WSS-80-4.
- [7] Peters, N 1983, 'Local Quenching Due to Flame Stretch and Non Premixed Turbulent Combustion' Combustion Science Technology **30**, pp. 1-17.
- [8] Peters, N 1984, 'Laminar Diffusion Flamelet Models in Non-Premixed Turbulent Combustion," Progress in Energy and Combustion Science, **10**, pp. 319-339.
- [9] Peters, N 2000, Turbulent Combustion, Cambridge University Press.
- [10] Bilger, RW 1980, "in: P.A. Libby, F.A. Williams (Eds.), Turbulent Reacting Flows, Springer-Verlag, Berlin, pp. 65-113.
- [11] Chen, H, Chen, S, Kraichnan, RH 1989, 'Probability Distribution of a Stochastically Advected Scalar Field', Physical Review Letters, **63**, pp. 2657-2660.
- [12] Pope SB 1991, 'Mapping Closures for Turbulent Mixing and Reaction 'Theoretical and Computational Fluid Dynamics **2**(5-6), pp.255-270.
- [13] Klimenko, AY 1990, 'Multi-component Diffusion of Various Admixtures in Turbulent Flow', Fluid Dynamics, **25**(3), pp. 327-334.
- [14] Bilger, RW 1993, 'Conditional Moment Closure for Turbulent Reacting Flow', Physics of Fluids, **5**, pp. 436-444.
- [15] Klimenko, AY, Bilger, RW 1999, 'Conditional Moment Closure for Turbulent Combustion', Progress in Energy and Combustion Science, **25**, pp. 595-687.
- [16] Klimenko, AY and Pope, SB 2003, 'The Modelling of Turbulent Reactive Flows based on Multiple Mapping Conditioning', Physical of Fluids, **15**, pp. 1907-1925.
- [17] Klimenko, AY 2004, 'Matching the Conditional Variance as a Criterion for Selecting Parameters in the Simplest Multiple Mapping Conditioning Models', Physical of Fluids, **16**, pp. 4754-4757.
- [18] Wandel, AP, 2005 'Development of Multiple Mapping Conditioning (MMC) for Application to Turbulent Combustion', PhD Thesis, University of Queensland, Australia.
- [19] Wandel, AP and Klimenko, AY, 2005, 'Multiple Mapping Conditioning Applied to Homogeneous Turbulent Combustion', Physics of Fluids, **17**, p. 128105.
- [20] Vogiatzaki, K, Kronenburg, A, Navarro-Martinez, S and Jones WP 2011 'Stochastic Multiple Mapping Conditioning for a Piloted, Turbulent Jet Diffusion Flame', Proceedings of the Combustion Institute **33**, pp. 1523-1531.
- [21] Ternat, F, Orellana, O and Daripa, P 2011 'Two Stable Methods with Numerical Experiments for Solving the Backward Heat Equation', Applied numerical Method, **61**, pp. 266-284.
- [22] Noor MM, Hairuddin, AA, Wandel AP and Yusaf, TF 2011 'Implementation of Conditional Moment Closure using Taylor Expansion and Finite Different Method', Int. Conf. of Mechanical Eng. Research (ICMER2011), 5-7 Dec, Malaysia, Paper ID:2011-151
- [23] Clarke, J, Wandel, AP and Mastorakos, E 2010 'Analysis of Data to Develop Models for Spray Combustion', Southern Region Engineering Conference (SREC), 11-12 Nov, Australia, Paper ID SREC2010-F2-1.
- [24] Curl, RL 1963, 'Dispersed Phase Mixing: I. Theory and Effects in Simple Reactors', AIChE Journal, **9**, pp. 175-181.

- [25] Levenspiel, O and Spielman, LA 1965, 'A Monte Carlo Treatment for Reacting and Coalescing Dispersed Phase Systems. Chemical Engineering Science, **20**, pp. 247-254.
- [26] Janicka, J, Kolbe, W, Kollmann, W 1979, 'Closure of the Transport Equation for the Probability Density Function of Turbulent Scalar Fields', Journal of Non-Equilibrium Thermodynamics, **4**, pp. 47-66.
- [27] Dopazo, C 1979, 'Relaxation of Initial Probability Density Functions in the Turbulent Convection of Scalar Fields', Physics of Fluids, **4(22)**, pp. 20-30.
- [28] Subramaniam, S and Pope, SB 1998, 'A Mixing Model for Turbulent Reactive Flows based on Euclidean Minimum Spanning Trees', Combustion and Flame, **115**, pp.487-514.
- [29] Villermaux, J., Devillon, J.C., 1972 'Representation de la Coalescence et de la Redispersion des Domaines de Segregation dans un uide par un Moduele d'Interaction Phenomenologique, Second International Symposium on Chemical Reaction Engineering, pp. 1-13.
- [30] Wandel, AP, 2011 A Stochastic Micromixing Model based on the Turbulent Diffusion Length Scale, 2011 Australian Combustion Symposium (ACS2011), Paper ID: ACS2011-20.
- [31] Noor, MM, Yusaf, TF and Wandel AP, 2011 Study of Random Particle Interactions for Analysis of Diffusion Lengths in Turbulent Combustion Modelling, 2011 Australian Combustion Symposium (ACS2011), Paper ID: ACS2011-36.
- [32] Liu, C & Karim, GA 2008, 'A simulation of the combustion of hydrogen in HCCI engines using a 3D model with detailed chemical kinetics', Int. J Hydrogen Energy, **33(14)**, pp. 3863-3875
- [33] Saravanan N and Nagarajan G 2010 'An experimental investigation on hydrogen fuel injection in intake port and manifold with different EGR rates', Energy and Env., **1(2)**, pp. 221-248.
- [34] Saravanan, N, Nagarajan, G, Sanjay, G, Dhanasekaran, C and Kalaiselvan, KM 2008, 'Combustion analysis on a DI diesel engine with hydrogen in dual fuel mode', Fuel, vol. **87**, no. 17-18, pp. 3591-3599.
- [35] Verhelst, S and Wallner, T 2009, 'Hydrogen-fuelled internal combustion engines', Progress in Energy and Combustion Science, **35(6)**, pp. 490-527
- [36] Mardani A, Tabejamaat S and Ghamari M. 2010 Numerical study of influence of molecular diffusion in the MILD combustion regime, Combust Theory Model, **14**, pp. 747-774
- [37] Mardani A and Tabejamaat S, 2010 Effect of hydrogen on hydrogenemethane turbulent non-premixed flame under MILD condition, Int. J Hydrog Energy, **35**, pp. 11324-11331
- [38] Wang F, Mi J, Li P and Zheng C. 2011 Diffusion flame of a CH<sub>4</sub>/H<sub>2</sub> jet in hot low-oxygen coflow, Int. J. Hydrogen Energy, **36**, pp. 9267-9277
- [39] Yu Y, Wang G, Lin Q, Ma C and Xing X 2010 'Flameless combustion for hydrogen containing fuels', Int. J Hydrogen Energy, **35**, pp. 2694-2697
- [40] Hollinger T and Bose T 2008 Hydrogen Internal Combustion Engine, Chapter 7a, in L'eon (ed.), Hydrogen Technology, Springer-Verlag, Berlin Heidelberg
- [41] Collatz, L 1966, 'The Numerical Treatment of Differential Equations', Springer Verlag, Berlin.
- [42] Krause, E. 1971 'Mehrstellen Verfahren zur Integration der Grenzschicht gleichungen', DLR Mitteilungen, **71(13)**, pp. 109-140.
- [43] Adam, Y 1975 'A Hermitian Finite Difference Method for the Solution of Parabolic Equations' Computational Mathematics Application, **1**, pp. 393-406.
- [44] Rubin, SG and Graves, RA 1975 'Viscous Flow Solutions with a Cubic Spline Approximation' Computational Fluid, **3**, pp. 1-36.
- [45] Hirsh, RS 1975, 'Higher Order Accurate Difference Solutions of Fluid Mechanics Problems by a Compact Differencing Scheme' Journal Computational Physics, **19**, pp. 20-109.
- [46] Ciment, M and Leventhal, SH 1975, 'Higher Order Compact Implicit Schemes for the Wave Equation' Mathematics Computational, **29**, pp. 885-944.
- [47] Adam, Y 1977 'Highly Accurate Compact Implicit Methods and Boundary Conditions', Journal Computational Physics, **24**, pp. 10-22.
- [48] Leventhal, SH 1980, 'The Operator Compact Implicit Method for Reservoir Simulation' Journal Society of Petroleum Engineering, **20**, pp. 120-128.

- [49] Peyret, R 1978 'A Hermitian Finite Difference Method for the Solution of the Navier–Stokes Equations', Proceedings First of the Conference on Numerical Methods in Laminar and Turbulent Flows, Pentech Press, Plymouth (UK) pp. 43-54.
- [50] Peyret, R and Taylor, TD 1982, 'Computational Methods for Fluid Flow', Springer Verlag, New York.
- [51] Lele, SK 1992, 'Compact Finite Differences with Spectral-like Resolution', Journal Computational Physics, **103**(1), pp. 16-42.
- [52] Rubin, SG and Khosla, PK 1977 'Polynomial Interpolation Method for Viscous Flow Calculations' Journal Computational Physics, **24**, pp. 217-246.
- [53] Chapra CS and Canale RP 2006, 'Numerical Methods for Engineers', McGraw Hill, 5<sup>th</sup> Edition, Singapore.
- [54] Griffiths DV and Smith IM 2006, 'Numerical Methods for Engineers' Chapman and Hall/CRC, 2<sup>nd</sup> Edition, New York.
- [55] D'Acunto, B, 2004, Computational Methods for PDE in Mechanics, World Scientific Publishing Co. Italy.
- [56] Kopriva DA and Kalias JH 1996, A Conservative Staggered-grid Chebyshev Multidomain Method for Compressible Flows, Journal of Computational Physics, **125**, pp. 244-261.
- [57] Yeung, RW and Ananthakrishnan, P 1992, Oscillation of a Floating Body in a Viscous Fluid, Journal of Engineering Mathematics, **26**, pp. 211-230.
- [58] Yeung, RW and Ananthakrishnan, P 1997, Viscosity and Surface-Tension Effects on Wave Generation by a Translating Body, Journal of Engineering Mathematics, **32**, pp. 257-280.
- [59] Hirsh, C 2007, Numerical Computation of Internal and External Flows: Fundamentals of Computational Fluid Dynamics, Butterworth-Heinemann, 1, Burlington, USA.
- [60] Courant, R, Friedrichs, K and Lewy, H 1928, Über Die Partiellen Differenzgleichungen Der Mathematischen Physik, Mathematische Annalen, **100**(1), pp 32-74.
- [61] Courant, R, Friedrichs, K and Lewy, H 1967, On the Partial Difference Equations of Mathematical Physics, English Translation from German 1928 Paper. IBM Journal, pp. 215-234.



**Nomenclature**

T	Temperature, K
D	Diffusivity
N	Scalar Dissipation Rate
V	Volume, m <sup>3</sup>
W	Chemical Source Term
Z	Mixture Fraction (a Conserved Scalar)
P	Favre Joint PDF of Composition
B	Constant (Function of $dt$ and $dz$ )
$E_a$	Activation Energy
$A, \beta$	Constants
$K, j$	Grid Point Involved in Space Difference
$L, i$	Grid Point Involved in Time Difference
$S_k$	Reaction Rate for Species k
$J_{ik}$	Molecular Diffusion Flux Vector
RANS	Reynolds Averaged Navier Stokes
CMC	Conditional Moment Closure
IEM	Interaction by Exchange with the Mean
DNS	Direct Numerical Simulation
MMC	Multiple Mapping Conditioning
CFD	Computational Fluid Dynamics
CFL	Courant-Friedrichs-Lewy
PDF	Probability Density Function
EMST	Euclidean Minimum Spanning Tree
MC	Modified Curl's model
TT	Total time for the simulation
YA	Air Mass Fraction
YH	Fuel Mass Fraction
$dt$	Time step size
$dz$	Step size in mixture fraction space
$u_i$	Favre Mean Fluid Velocity Vector
$\psi$	Composition Space Vector
$u_i''$	Fluid Velocity Fluctuation Vector
$\dot{\omega}_i$	Net Formation Rate per Unit Volume
$\nu$	Kinematic Viscosity,
$\alpha$	Thermal Diffusivity, m <sup>2</sup> /s
$\phi$	Particle Composition
$k$	Thermal Conductivity, W/mK
$k_j$	Arrhenius Reaction Rate Coefficient
$\rho$	Density or Mean Fluid Density, kg/m <sup>3</sup>
R	Universal Gas Constant (8.31431 kJ kmol <sup>-1</sup> K <sup>-1</sup> )
$\bar{w}$	Molecular Weight of a Gas Mixture
$\langle \quad \rangle$	Ensemble Average
$\langle Y Z \rangle$	Mass Fraction of Fuel
$\langle N Z \rangle$	Conditional Scalar Dissipation
$\langle W Z \rangle$	Conditional Chemical Source Term
$\langle S Z \rangle$	Conditional Generation Due to Droplet Evaporation

## Appendix A: Part of FORTRAN code for explicit method

```

YH(:,1) = 0.0   Comment: Initial Condition
YH(L,1) = 1.0
YA(1,:) = 1.0
YA(L,1) = 0.0
Comment: Main Calculation
Do j=1, K
Do i=2, L
YH(i,j+1) = ((1-(2*B))*YH(i,j)) + (B*YH(i+1,j)) + (B*YH(i-1,j))
YA(i,j+1) = ((1-(2*B))*YA(i,j)) + (B*YA(i+1,j)) + (B*YA(i-1,j))
End Do
YH(1,j+1)=0   Comment: Boundary Condition
YH(L,j+1)=1
YA(1,j+1)=1
YA(L,j+1)=0
End Do

```

## Appendix B: Part of FORTRAN code for implicit method

```

A(1,1) = 0.0   Comment: Initial Condition
A(2,1) = 1.0
A(1,2) = 0.0
Do i=2, dz-1
A(3,i-1) = - B
A(2,i) = 1.0 + 2.0 * B
A(1,i+1) = - B
End Do
A(3,dz-1) = 0.0
A(2,dz) = 1.0
A(3,dz) = 0.0
Comment: Factor the matrix
Call MatrixC (dz,a,b,FF)
Do j = 2, dt
Call YH (z_min,z_max,t_min,t(j),B(1))
B(2:dz-1) = YH(2:dz-1,j-1)
Call YA (z_min,z_max,t_min,t(j),B(dz))
WW = 0
Call MatrixD (dz,a,b,WW)
YH(1:dz,j) = B(1:dz)
End Do
Comment: Subroutine for matrix
Do i = 1, n-1
If (P(2,i) .eq. 0.0 ) then
info = i
Write (*, '(P)') 'MatrixD - error'
Return
End If
P(3,i) = P(3,i) / P(2,i)
P(2,i+1) = P(2,i+1) - P(3,i) * a(1,i+1)
End Do

```